Contribution from the Departamento de Química Inorgánica, Facultad de Ciencias, Universidad de Málaga, Apartado 59, 29071 Málaga, Spain, and Instituto de Ciencia de los Materiales de Aragón, CSIC—Universidad de Zaragoza, Facultad de Ciencias, 50009 Zaragoza, Spain

Characterization of Manganese(III) Dihydrogen Triphosphate Dihydrate, $H_2MnP_3O_{10}\cdot 2H_2O$

Miguel A. G. Aranda,[1] Jesus Chaboy,[2] and Sebastian Bruque*,[1]

Received September 10, 1990

Manganese(III) dihydrogen triphosphate dihydrate, $H_2MnP_3O_{10}\cdot 2H_2O$, has been studied by different techniques. TGA–DTA curves for this compound are shown, and the different steps in the heating process are explained. The most important bands of the IR spectrum are assigned, and the presence of the oxonium ion is detected. The diffuse-reflectance spectrum is discussed, an important Jahn–Teller effect being observed. Results from the analysis of the EXAFS spectrum show a distorted octahedral environment of manganese with Mn–O distance 4 × 1.86, 2.09, and 2.24 Å. Diffuse-reflectance spectral data are in agreement with the manganese environment obtained from the EXAFS study.

Introduction

We are currently undertaking a detailed synthetic, spectroscopic, and reactivity study of the manganese(III) phosphates. As part of this study, we have recently investigated $MnPO_4\cdot 1.3H_2O$ by spectroscopic methods.[3]

Little synthetic and structural work has been reported for the Mn_2O_3–P_2O_5–H_2O system, and only the structures of the mixed-valence mineral bermanite ($Mn_3(PO_4)_2(OH)_2\cdot 4H_2O$), $Mn(PO_3)_3$, and $MnPO_4\cdot H_2O$ are well-known.[4-6] Two new layer-type phosphates involving Mn(III) have been recently synthesized: $KMn_2O(PO_4)(HPO_4)$ and $NH_4Mn_2O(PO_4)(HPO_4)\cdot H_2O$.[7,8]

The X-ray powder diffraction pattern of $H_2MnP_3O_{10}\cdot 2H_2O$[9] shows that it belongs to the series of isomorphous tripolyphosphates $H_2M^{III}P_3O_{10}\cdot 2H_2O$[10] where M^{III} = Al, Ga, V, Cr, or Fe, but the unit cell and structure of this series are unknown. These compounds are inorganic ion exchangers, and the protons may be replaced by univalent metal cations (Na or Cs).[11] The proton-exchanged compounds sorb basic substances such as ammonia or hydrazine.[12] These properties must be due to the presence of accessible acidic groups in the structure.

The state and structure of the proton-containing groups in aluminum dihydrogen triphosphate dihydrate have been refined by infrared spectroscopic and broad-line NMR methods.[13] The obtained structure is an equilateral triangle with the proton of the oxyhydryl groups at the apex, while the water protons are at the base. There is a thermodynamic equilibrium between this structure and the symmetrical oxonium ion.

The interest for study of manganese(III) dihydrogen triphosphate dihydrate is due to the fact that this class of compounds would be good protonic conductors because of the presence of oxonium ions in its structure and, furthermore, because of the intercalation reactions that can occur in these materials.

This paper presents the study of $H_2MnP_3O_{10}\cdot 2H_2O$ by different techniques. Thermal analysis helps to measure the water content and shows the condensation of the POH groups and the reduction of Mn(III) to Mn(II) in the heating process. Infrared spectroscopy shows mainly the different proton-containing groups in the structure. Extended X-ray absorption fine structure (EXAFS) spectroscopy provides information on the local structural environment of the manganese, and these results are compared with data obtained from the diffuse-reflectance UV–visible–near-IR spectrum.

Experimental Section

$H_2MnP_3O_{10}\cdot 2H_2O$ was synthesized by Selevich et al.[9] from phosphoric acid and $MnCl_2\cdot 4H_2O$, in the presence of nitric acid in the temperature range 210–240 °C.

Others synthetic designs were tested in order to remove the quasi-amorphous phase that accompanies this compound. As phosphorus sources we used phosphoric acid, polyphosphoric acid (84% P_2O_5), and phosphorus(V) oxide, P_2O_5. As manganese sources, manganese(II) carbonate, manganese(III) oxide, and manganese(IV) oxide were tested. The P/Mn ratio, temperature, reaction time, and solvents were varied. Although attempts to remove this amorphous phase were all unsuccessful, the following synthesis gave the best ratio between the well-crystalline and quasi-amorphous phases.

Mn_2O_3 (2 g) and polyphosphoric acid (84% P_2O_5, 15 g), with a P/Mn ratio of 7, were heated at 180 °C for 3 days. The product was filtered out, washed three times (20 mL) with water and finally with 20-mL portions of acetone, until the washing liquids were colorless, and then dried at room temperature. The sample shows an X-ray powder diffraction pattern similar to that published by Selevich et al.[9]

Chemical analysis was carried out by methods described elsewhere.[3] Anal. Calcd for $H_2MnP_3O_{10}\cdot 2H_2O$: Mn_2O_3, 22.8; P_2O_5, 61.6; H_2O, 14.8. Found: Mn_2O_3, 22.6; P_2O_5, 61.0; H_2O, 15.5.

The oxidation state of the manganese was obtained by dissolving the sample in a solution of potassium iodide and hydrochloric acid. The iodine liberated by the reduction of the manganese to Mn(II) was titrated with $Na_2S_2O_3$ solution, in the presence of starch. The manganese oxidation state was found to be 2.97.

X-ray microprobe analysis of the product, by the "ratio method"[14] in a JEOL 2000FX electron microscope, confirmed a P/Mn ratio of 3, with $MnPO_4\cdot H_2O$ used as a standard. Microcrystals were not found with a ratio P/Mn different from 3 within the standard deviation of the measurement.

Thermal analyses (TGA and DTA) were carried out in air on a Rigaku Thermoflex apparatus at a heating rate of 10 K·min^{-1} with calcined Al_2O_3 as the standard reference. Infrared spectra were recorded on a Perkin-Elmer 883 spectrometer in the spectral range from 4000 to 200 cm^{-1} using a dry KBr Pellet containing 2% sample. The diffuse-reflec-

* To whom correspondence should be addressed.

(1) Universidad de Málaga
(2) CSIC—Universidad de Zaragoza
(3) Aranda, M. A. G.; Bruque, S. *Inorg. Chem.* **1990**, *29*, 1334.
(4) Kampk, A. R.; Moore, P. B. *Am. Mineral.* **1976**, *61*, 1241.
(5) Bagieu-Beucher, M. *Acta Crystallogr.* **1978**, *B34*, 1443.
(6) Lightfoot, P.; Cheetham, A. K.; Sleight, A. W. *Inorg. Chem.* **1987**, *26*, 3544.
(7) Lightfoot, P.; Cheetham, A. K.; Sleight, A. W. *J. Solid State Chem.* **1988**, *73*, 325.
(8) Lightfoot, P.; Cheetham, A. K. *J. Solid State Chem.* **1988**, *78*, 17.
(9) Selevich, A. F.; Lyutsko, V. A. *Zh. Neorg. Khim.* **1984**, *29*, 629; *Russ. J. Inorg. Chem.* (*Engl. Transl.*) **1984**, *29*, 364.
(10) (a) d'Yvoire, F. *Bull. Soc. Chim. Fr.* **1962**, 1224. (b) Remy, P.; Fraissard, J.; Boulle, A. *Bull. Soc. Chim. Fr.* **1972**, 2213. (c) Lyutsko, V. A.; Selevich, A. F. *Zh. Neorg. Khim.* **1983**, *28*, 923; *Russ. J. Inorg. Chem.* (*Engl. Transl.*) **1983**, *28*, 521. (d) Lyutsko, V. A.; Khansen, E.; Selevich, A. F.; Petrovskaya, L. I. *Zh. Neorg. Khim.* **1985**, *30*, 598; *Russ. J. Inorg. Chem.* (*Engl. Transl.*) **1985**, *30*, 336. (e) Lyutsko, V. A.; Selevich, A. F.; Lyakhov, A. S. *Zh. Neorg. Khim.* **1988**, *33*, 1723; *Russ. J. Inorg. Chem.* (*Engl. Transl.*) **1988**, *33*, 980.
(11) Lyutsko, V. A.; Nikanovich, M. V.; Lapko, K. N.; Tikavyi, V. F. *Zh. Neorg. Khim.* **1983**, *28*, 1949; *Russ. J. Inorg. Chem.* (*Engl. Transl.*) **1983**, *28*, 1105.
(12) (a) Lyutsko, V. A.; Selevich, A. F. *Zh. Neorg. Khim.* **1985**, *30*, 1800; *Russ. J. Inorg. Chem.* (*Engl. Transl.*) **1985**, *30*, 1023. (b) Lyutsko, V. A.; Tuchkovskaya, A. V. *Zh. Neorg. Khim.* **1985**, *30*, 2259; *Russ. J. Inorg. Chem.* (*Engl. Transl.*) **1985**, *30*, 1284. (c) Lyutsko, V. A.; Tuchkovskaya, A. V.; Shifrina, A. L. *Zh. Neorg. Khim.* **1987**, *32*, 2649; *Russ. J. Inorg. Chem.* (*Engl. Transl.*) **1987**, *32*, 1541.
(13) Lapko, K. N.; Makatun, V. N.; Ugolev, I. I. *Zh. Neorg. Khim.* **1980**, *25*, 1688; *Russ. J. Inorg. Chem.* (*Engl. Transl.*) **1980**, *25*, 938.
(14) Cliff, G.; Lorimer, G. W. *J. Microsc.* (*Oxford*). **1975**, *103*, 207.

0020-1669/91/1330-2394$02.50/0

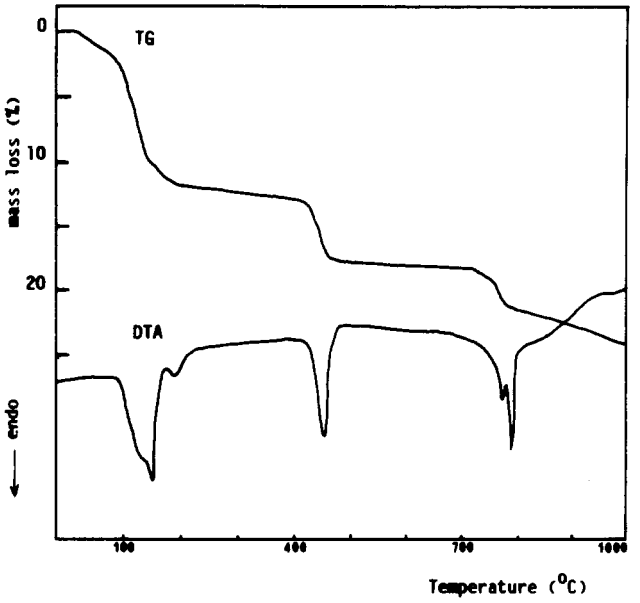

Figure 1. Thermal analysis (TGA and DTA) for $H_2MnP_3O_{10}\cdot 2H_2O$.

tance spectrum was obtained on a Shimadzu UV-3100 spectrophotometer using an integrating sphere and $BaSO_4$ as a reference blank. Powder X-ray diffraction patterns were recorded on an automatic Siemens D-501 diffractometer using graphite-monochromated Cu Kα radiation.

The EXAFS spectrum was recorded at room temperature for the K absorption edge of the Mn atom, with the use of synchrotron radiation at Frascati, the monochromator was a channel-cut Si(111) single crystal, and the operating conditions were an energy of 1.5 GeV and a maximum beam current of 70 mA. Analysis of the data was performed with a VAX 8530 computer at Malaga University. Established procedures were used to extract the EXAFS oscillation from the absorption data.[15] The background-subtracted EXAFS was then converted into k-space and weighted by k^3 in order to compensate for the disminishing amplitude at high k due to the decay of the photoelectron wave. The data were Fourier-filtered to include the first two shells, a cutoff which can be made without introducing a large truncation error. Analysis of the Fourier-filtered EXAFS was carried out by using the program EXCURV88,[16] which is based on spherical-wave theory.[17] An ab initio approach was used to calculate initial values for the atomic phase shifts, as previously described.[18] Multiple-scattering calculations were carried out within EXCURV by defining the geometry of the array Mn–O–P and then submitting a background job by using the program EXFIT88. The estimated levels of accuracy in our refinements are as follows: distances, ±0.02 Å; Debye–Waller factor, ±30%; angles, ±5°.

Results and Discussion

The series of isomorphous triphosphates $H_2M^{III}P_3O_{10}\cdot 2H_2O$ where M^{III} = Al, Ga, Mn, V, Cr, or Fe have an unknown structure and an unindexed unit cell. This is due to the fact that they are always obtained as mixtures of phases, one major phase with very sharp and high-intensity peaks and another minor phase with broader peaks of lower intensity.

As the X-ray microanalysis gives a constant P/Mn ratio of 3 for all analyzed microcrystals, the minor phase may be due to a different degree of hydration or a quasi-amorphous phase that accompanies this series.

We are at present trying to resolve the full crystal structure from high-resolution synchrotron X-ray powder diffraction data.

The TGA–DTA curves for manganese(III) dihydrogen triphosphate dihydrate are shown in Figure 1. The DTA curve shows three different regions. The first is composed of three endothermic effects centered at 120, 150, and 185 °C. This set

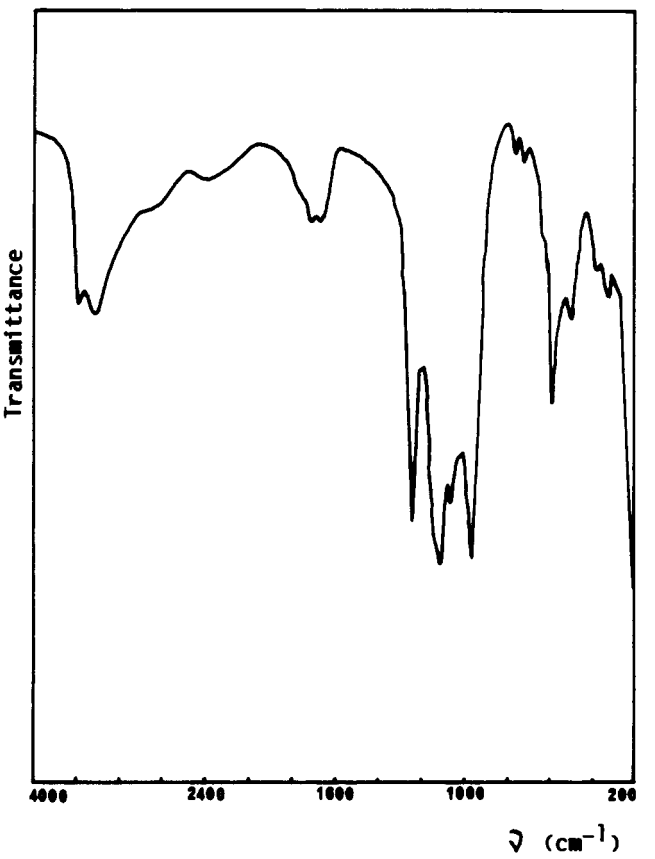

Figure 2. Infrared spectrum of $H_2MnP_3O_{10}\cdot 2H_2O$.

of endotherms is due to the loss of the two water molecules. The loss of weight calculated is 10.4%, and found, 9.8%.

$$H_2MnP_3O_{10}\cdot 2H_2O \rightarrow H_2MnP_3O_{10} + 2H_2O$$

The second region consists of one endotherm at 450 °C and is associated with the condensation of the hydrogen polyphosphate groups. The loss of weight calculated is 5.2%, and found, 5.7%.

$$H_2MnP_3O_{10} \rightarrow Mn(PO_3)_3 + H_2O$$

$Mn(PO_3)_3$ was identified unequivocally by its X-ray powder pattern.[5] The third region is composed of two endothermic effects at 770 and 785 °C. These are due to the reduction of Mn(III) to Mn(II) and the consequent release of oxygen and the loss of P_2O_5 to yield manganese(II) tetrametaphosphate, which was identified by its powder diffraction pattern.[19]

$$2Mn(PO_3)_3 \rightarrow Mn_2P_4O_{12} + \tfrac{1}{2}O_2 + P_2O_5$$

The IR spectrum of $H_2MnP_3O_{10}\cdot 2H_2O$ is shown in the Figure 2. Four bands appear in the region of hydroxyl stretching. The two bands centered at 3560 and 3440 cm^{-1} suggest the presence of at least two different kinds of H_2O. The first, which is sharper and at higher frequency, corresponds to a less strongly hydrogen-bonded water molecule, and the second, which is broader, corresponds to a strongly hydrogen-bonded water. The band located near 2950 cm^{-1} appears as a shoulder and may be attributed to the stretching vibrations of the oxonium ion (H_3O^+).[20] The last band near 2345 cm^{-1} is assigned to PO–H stretching,[21] or overtone bands of the PO_4 stretching bands.

Two bands may be seen in the H–O–H bending region, centered at 1700 and 1655 cm^{-1}. The first is assigned to the deformation vibration of the H_3O^+, and the second is due to the bending vibration of the H_2O. These wide bands between 1800 and 1600

(15) EXCALIB and EXBACK programs available from Daresbury Laboratory.
(16) Binsted, N.; Gurman, S. J.; Campbell, J. SERC Daresbury Laboratory EXCURV88 program, 1988.
(17) (a) Lee, P. A.; Pendry, J. B. *Phys. Rev. B* **1975**, *11*, 2795. (b) Gurman, S. J.; Binsted, N.; Ross, I. *J. Phys. C: Solid State Phys.* **1984**, *17*, 578.
(18) Binsted, N.; Cook, S. L.; Evans, J.; Greaves, G. N.; Price, R. J. *J. Am. Chem. Soc.* **1987**, *109*, 3669.
(19) Joint Committee on Powder Diffraction Standards. *Index to the Powder Diffraction Files*; ASTM: Philadelphia, PA, 1982.
(20) Remy, P.; Fraissard, J.; Boulle, A. *Bull. Soc. Chim. Fr.* **1968**, 2222.
(21) Casañ, N.; Amorós, P.; Ibáñez, R.; Martinez-Tamayo, E.; Beltrán-Porter, A.; Beltrán-Porter, D. *J. Inclusion Phenom.* **1988**, *6*, 193.

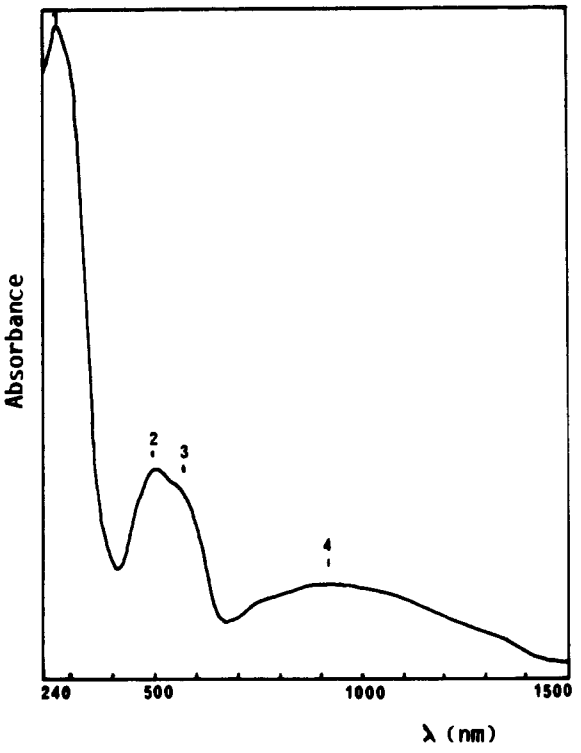

Figure 3. Diffuse-reflectance UV–vis–near-IR spectrum of $H_2MnP_3O_{10}\cdot 2H_2O$.

Table I. Diffuse-Reflectance Data for $H_2MnP_3O_{10}\cdot 2H_2O$

band	absorption		assignt
	nm	cm^{-1}	
1	255	39 210	charge transfer
2	481	20 790	$^5B_{1g} \rightarrow {}^5E_g$
3	569	17 575	$^5B_{1g} \rightarrow {}^5B_{2g}$
4	895	11 173	$^5B_{1g} \rightarrow {}^5A_{1g}$

cm^{-1} are usually related to protonic conductivity phenomena.[22]

The absorption band involving the triply degenerate stretching vibration $\nu_3(PO_4)$ is split when it interacts with other PO_4 tetrahedra. Therefore, the set of three bands situated at 1235, 1109, and 1056 cm^{-1} may be assigned to $\nu_3(PO_4)$ stretching vibrations.[23] The band centered at 963 cm^{-1} is assigned to the $\nu_1(PO_4)$ vibration. This mode is only active in the Raman spectrum in T_d symmetry, but with lowering of symmetry it becomes active in the IR spectrum.[24] The weak bands close to 765 and 720 cm^{-1} are assigned to the δ(P–O–P) asymmetric and symmetric bending vibrations, respectively. The shoulder near 620 cm^{-1} is assigned to δ(Mn–O–P). The high-intensity bands situated at 581 and 496 cm^{-1} have been assigned to $\nu_4(PO_4)$ and ν(Mn–OP), respectively, according to the literature.[3,25]

In the diffuse-reflectance spectrum (Figure 3), one sees a set of four bands, while Mn(III), which is a d^4 ion, in an octahedral environment should show only one band due to the $^5E_g \rightarrow {}^5T_{2g}$ transition. The first band centered at 255 nm is too strong to be due to a d–d transition, and as it lies in the ultraviolet region, is assigned as an oxygen-to-Mn(III) charge-transfer band. The appearance of three bands in the visible region can only be explained by a Jahn–Teller effect. Table I lists values of the absorption maxima and their assignments. The maxima of the second and third bands have been obtained from their second derivatives, since they are partially overlapping.

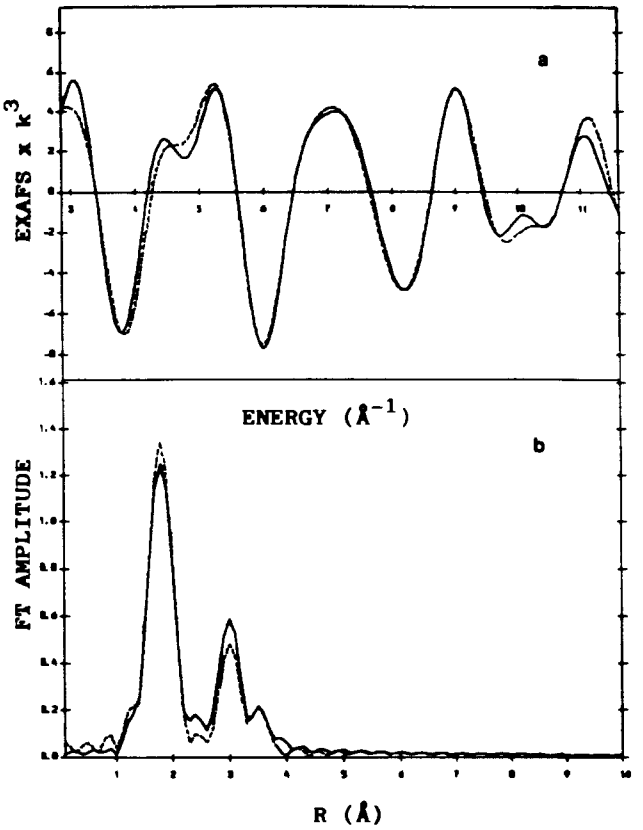

Figure 4. (a) Observed (—) and calculated (---) Fourier-filtered EXAFS data and (b) the corresponding Fourier transforms for $H_2MnP_3O_{10}\cdot 2H_2O$.

The *Dq* parameter for this compound, read from the spectrum, has the value 1757 cm^{-1} because 10*Dq* coincides with the energy of the third transition, $^5B_{1g} \rightarrow {}^5B_{2g}$. Analogous values are found for other complexes containing Mn(III), for example, 1770 cm^{-1} for $MnPO_4\cdot 1.3H_2O$, 1780 cm^{-1} for $[MnF_6]^{3-}$, and 1667 cm^{-1} for $Mn(DMSO)_6^{3+}$.[3,26]

The ground-state splitting (GSS) coincides with the fourth band, and the excited-state splitting (ESS) is the difference between the second and the third bands. Thus, GSS assumes a value of 11 173 cm^{-1}, and ESS, a value of 3215 cm^{-1}. The assignments lead to the following values of McClure parameters:[27] $d\sigma = -4190$ cm^{-1} and $d\pi = -1607$ cm^{-1}. These are of the same order as those found in the literature.[26,28] These parameters are consistent with an elongated tetragonal distortion and a small amount oxygen-to-manganese π-bonding.[3]

The values of the crystal field splitting energy for manganese(III) dihydrogen triphosphate dihydrate and for manganese(III) phosphate hydrate are quite close, 17 570 and 17 700 cm^{-1}, respectively. This is natural because in the two cases there is a manganese(III) in a distorted octahedral environment of oxygen atoms, but the values for $d\sigma$ and $d\pi$ in these compounds are quite different: −4190 and −1607 cm^{-1} for $H_2MnP_3O_{10}\cdot 2H_2O$ and −5640 and 2140 cm^{-1} for $MnPO_4\cdot 1.3H_2O$. These are differences that arise from the octahedral environment being more distorted for $MnPO_4\cdot 1.3H_2O$ than for $H_2MnP_3O_{10}\cdot 2H_2O$, and the oxygen-to-manganese π-bonding is also greater, perhaps because Mn–O–Mn chains are present only in the first compound.

For the EXAFS study the manganese environment in $H_2MnP_3O_{10}\cdot 2H_2O$ was described as a series of shells. The theoretical EXAFS spectrum was calculated from the environment of

(22) Pham-Thi, M.; Colomban, P.; Novak, A. *J. Phys. Chem. Solids* **1985**, *46*, 565.
(23) Lelong, B. *Ann. Chim.* **1964**, *9*, 229.
(24) Nakamoto, K. In *Infrared Spectra of Inorganic and Coordination Compounds*, 2nd ed.; Wiley, J. S., Ed.; Wiley-Interscience: New York, 1970.
(25) Farmer, V. C. *The Infrared Spectra of Minerals*; Mineralogical Society: London, 1974.
(26) Lever, A. B. P. *Inorganic Electronic Spectroscopy*, 2nd ed.; Elsevier Science Publishers: Amsterdam, 1984.
(27) McClure, D. S. *Advances in the Chemistry of the Coordination Compounds*; Macmillan: New York, 1961.
(28) Hush, N. S.; Hobbs, J. M. In *Progress in Inorganic Chemistry*; Cotton, F. A., Ed.; Wiley-Interscience: New York, 1968; p 259.

Table II. Radial Distribution of Atoms about Mn and Mn–O–P Angles in $H_2MnP_3O_{10}\cdot 2H_2O$

atom type	coordn no.	radial dist, Å	Debye–Waller factor ($2\sigma^2$), Å^2
O(1)	4	1.86	0.007
O(2)	1	2.24	0.007
O(3)	1	2.09	0.007
P(1)	4	3.14	0.008
P(2)	1	3.37	0.008
P(3)	1	3.27	0.008

Mn–O–P	angle, deg
Mn–O(1)–P(1)	135
Mn–O(2)–P(2)	125
Mn–O(3)–P(3)	130

manganese in $MnPO_4\cdot H_2O$.[6] The octahedral coordination of oxygens is distorted axially, because both compounds show a Jahn–Teller effect, although in the second compound it is larger.

Values of Mn–O distances and Debye–Waller factors were refined to obtain the best fit between theory and experiment. Then, calculations were performed for phosphorus in the second shell and for multiple scattering within the three-atom array Mn–O–P to obtain the refined Mn–O–P angles.

Refinement of the radial distances (Mn–O and Mn···P), Debye–Waller factors, and the Mn–O–P angles led to a very satisfactory level of agreement between the observed and calculated spectra and its Fourier transform, as illustrated in Figure 4. The values of the refined parameters are listed in Table II.

The Mn–O–P framework consists of axially distorted MnO_6 octahedra that share all six corners with PO_4 tetrahedra. The observed bond distances 4 × 1.86, 1 × 2.09, and 1 × 2.24 Å are similar to those in other manganese(III) oxide systems: Mn_2O_3,[29] which has 4 × 1.90 and 2 × 2.24 Å; $NaMnO_2$,[30] with 4 × 1.92 and 2 × 2.40 Å; $MnPO_4\cdot H_2O$,[6] having 2 × 1.89, 2 × 1.91, and 2 × 2.28 Å; and $Mn(PO_3)_3$,[5] with 2 × 1.88, 2 × 1.91, and 2 × 2.16 Å.

The P–O distances may be calculated from the Mn–O and Mn–P distances and the angles obtained from multiple-scattering calculations. The manganese(III) environment with all distances (Å) and angles (deg) obtained from the EXAFS study is shown in I.

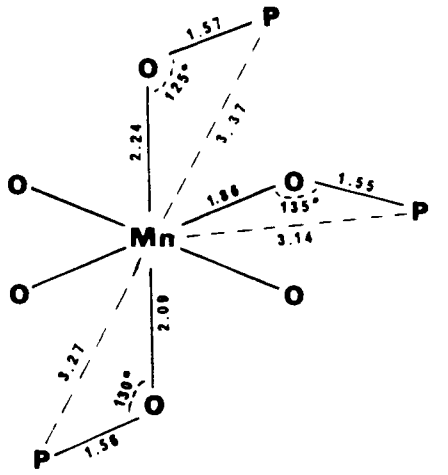

I

The manganese(III) environment confirms the Jahn–Teller effect that is seen in the diffuse-reflectance spectrum. This environment is less distorted than that observed in manganese(III) orthophosphate hydrate,[6] in agreement with the diffuse-reflectance results.[3]

The layered framework of this compound has been proved from a butylamine intercalation experiment in the vapor phase. The basal spacing increases from 7.77 to 15.45 Å after *n*-butylamine intercalation. However, only the first reflection line is sharp and the X-ray powder pattern at high angles (2θ) is poor.

Acknowledgment. We acknowledge helpful discussions with Dr. J. P. Attfield (University of Oxford, U.K.) and Dr. J. Garcia-Ruiz (Universidad de Zaragoza, Spain) and thank the Comisiôn Interministerial de Ciencia y Tecnologia (CICYT, Spain) and Istituto Nazionale di Fisica Nucleare (INFN, Italy) for use of the facility at Frascati. M.A.G.A. and J.C. also wish to thank the Ministerio de Educación y Ciencia (Spain) for the provision of studentships.

(29) Geller, S. *Acta Crystallogr.* **1971**, *B27*, 821.
(30) Jansen, M.; Hoppe, R. *Z. Anorg. Allg. Chem.* **1973**, *399*, 163.

Contribution from the Department of Chemistry, University of South Carolina, Columbia, South Carolina 29208

Luminescence Studies of Tris[dihydrobis(1-pyrazolyl)borato]terbium(III)

Daniel L. Reger,* Pi-Tai Chou,* Shannon L. Studer, Steven J. Knox, Marty L. Martinez, and William E. Brewer

Received April 27, 1990

The luminescence spectra and dynamics of $[H_2B(pz)_2]_3Tb$ have been studied at different temperatures, in the solid phase and in various solvents. Analysis of the data for the crystalline sample based on the electron dipole selection rules reveals effective C_3 symmetry about the terbium atom. Thus, the luminescence spectra are those expected for the trigonal-prismatic arrangement of the nitrogen donor atoms but influenced by the three weak BH···Tb three-center bonds to each of the rectangular faces. Similar luminescence spectra are observed for $[H_2B(pz)_2]_3Tb$ in CH_2Cl_2 and toluene solutions. In donor solvents, complexation of $[H_2B(pz)_2]_3Tb$ with the solvent molecules changes the lifetime and the spectral feature of the luminescence, indicating a change in the coordination environment about the terbium atom.

Introduction

We have recently been exploring the chemistry of early metals and the lanthanides using the versatile poly(pyrazolyl)borate ligand system.[1] A particularly interesting complex that we have prepared and carefully characterized by multinuclear NMR and single crystal X-ray crystallography is $[H_2B(pz)_2]_3Y$ (**1**, pz = pyrazolyl ring).[1a] In the solid state, the six nitrogen donor atoms of the bis(pyrazolyl)borate ligands are arranged in a trigonal-prismatic array. In addition, the six-membered YN_4B rings are oriented in a puckered boat configuration that brings one of the hydrogen atoms on each of the three boron atoms in close proximity to the yttrium metal, indicating the formation of three three-center, two-electron BH···Y bonding interactions (agostic bonds). A

(1) (a) Reger, D. L.; Lindeman, J. A.; Lebioda, L. *Inorg. Chem.* **1988**, *27*, 1890. (b) Reger, D. L.; Lindeman, J. A.; Lebioda, L. *Ibid.* **1988**, *27*, 3923. (c) Reger, D. L.; Knox, S. L.; Lindeman, J. A.; Lebioda, L. *Ibid.* **1990**, *29*, 416.

0020-1669/91/1330-2397$02.50/0